Global and regional drivers of power plant CO_2 emissions over the last three decades

Xinying Qin[a], Dan Tong[a,*], Fei Liu[b], Ruili Wu[c], Bo Zheng[d], Yixuan Zheng[e], Jun Liu[f], Ruochong Xu[a], Cuihong Chen[a], Liu Yan[a], Qiang Zhang[a]

[a] Department of Earth System Science, Ministry of Education Key Laboratory for Earth System Modeling, Institute for Global Change Studies, Tsinghua University, Beijing 100084, China
[b] State Key Joint Laboratory of Environment Simulation and Pollution Control, School of Environment, Tsinghua University, Beijing, 100084, China
[c] State Environmental Protection Key Laboratory of Quality Control in Environmental Monitoring, China National Environmental Monitoring Centro, Beijing 100012, China
[d] Institute of Environment and Ecology, Tsinghua Shenzhen International Graduate School, Tsinghua University, Shenzhen, 518055, China
[e] Center of Air Quality Simulation and System Analysis, Chinese Academy of Environmental Planning, Beijing 100012, China
[f] Department of Environmental Engineering, School of Energy and Environmental Engineering, University of Science and Technology Beijing, Beijing 100083, China

[*]*Correspondence to*: Dan Tong (dantong@tsinghua.edu.cn)

Abstract

The past three decades have witnessed the dramatic expansion of global biomass- and fossil fuel-fired power plants, but the tremendously diverse power infrastructure shapes different spatial and temporal CO_2 emission characteristics. Here, by combining Global Power plant Emissions Database (GPED v1.1) constructed in this study and the previously developed China coal-fired power Plant Emissions Database (CPED), we analyzed global and regional changes in generating capacities, age structure, and CO_2 emissions by fuel type and unit size, and further identified the major driving forces of these global and regional structure and emission trends over the past 30 years. Accompanying the growth of fossil fuel- and biomass-burning installed capacity from 1,774 GW in 1990 to 4,139 GW in 2019 (a 133.3% increase), global CO_2 emissions from the power sector relatively increased from 7.5 Gt to 13.9 Gt (an 85.3% increase) during the same period. However, diverse developments and transformations of regional power units in fuel types and structure characterized various regional trends of CO_2 emissions. For example, in the United States and Europe, CO_2 emissions from power plants peaked before 2005, driven by the utilization of advanced electricity technologies and the switches from coal to gas fuel at the early stage. It is estimated the share of identified low-efficiency coal power capacity decreased to 4.3% in the United States and 0.6% in Europe with respectively 2.1% and 13.2% thermal efficiency improvements from 1990-2019. In contrast, CO_2 emissions in China, India, and the rest of world are still steadily increasing because the growing demand for electricity is mainly met by developing carbon-intensive but less effective coal power capacity. The index decomposition analysis (IDA) to identify the multi-stage driving forces on the trends of CO_2 emissions further suggests different global and regional characteristics. Globally, the growth of demand mainly drives the increase of CO_2 emissions for all stages (i.e. 1990-2000, 2000-2010 and 2010-2019). Regional results support the critical roles of thermal efficiency improvement (accounting for 20% of the decrease in CO_2 emissions) and fossil fuel mix (61%) in preventing CO_2 emission increases in the developed regions (e.g., the United States and Europe). The decrease of fossil fuel share gradually demonstrates its importance in carrying the positive effects on curbing emissions in the most of regions, including the developing economics (i.e. China and India) after 2010 (accounting for 46% of the decrease in CO_2 emissions). Our results highlight the contributions of different driving forces to emissions have significantly changed over the past 30 years, and this comprehensive analysis indicates that the structure optimization and transformations of power plants is paramount importance to curb or further reduce CO_2 emissions from the power sector in the future.

Keywords

Global power units
CO_2 emission trends
Power structure evolutions
Emission drivers

1 Introduction

Carbon dioxide (CO_2) emissions from fossil fuel burning are recognized as one of major causes of the global temperature increase of approximately 1°C since the beginning of the industrial era [1–3]. As the largest source of anthropogenic CO_2 emissions, the power sector accounted for 37% of global total anthropogenic CO_2 emissions in 2019 compared to 30% in 1990, and it plays an increasingly critical role in global carbon commitment and climate change mitigation [4–6]. Global fossil fuel power generation grew from 7,609 TWh in 1990 to 17,642 TWh in 2019, at an annual average rate of 3.0%, driven by population growth and economic development [7]. Global CO_2 emissions from the power sector thus have increased rapidly with the growth in demand for electricity generation in recent decades, and higher growth rates of electricity generation and power plant CO_2 emissions have been observed in many developing countries [8–10]. However, the growth of power generation is likely to continue with the increase in electrification and the substitution of direct fuel consumption in end-use sectors with electricity [11–15]. The rapid decoupling of global power generation demand from its CO_2 emissions is a necessary step in the coming decades to achieve the Paris Agreement of limiting the temperature increase to well below 2 ℃ above pre-industrial levels and pursuing 1.5 ℃ [16–18].

Over the past few decades, both developed and developing countries have made efforts to reduce CO_2 emissions from the power sector [19–21]. A large number of national climate and energy policies have been implemented to reduce CO_2 emissions [22–26], playing a vital role in tackling climate change [27,28]. For example, on the one hand, climate and energy policies of improving the thermal efficiency of fossil fuel power plants have been proven effective in reducing CO_2 emissions of power plants in developed countries [29–32]. On the other hand, studies have also proven that fuel switching from coal to natural gas has also helped decrease CO_2 emissions from the power sector [33–35]. Although these studies have partly analyzed regional and national drivers of power plant CO_2 emissions, systematically assessing both global and regional drivers of power plant CO_2 emissions are restricted by global uniform high-resolution power plants emissions database. Further, comprehensively understanding the global and regional drivers of power plant emissions could reveal how climate and energy policies can help decarbonize global power sector and support the future exploration of deep mitigation.

A global high-resolution CO_2 emissions dataset of power plants is fundamental for assessing the historical multi-scale evolution of generating capacities and power structures and exploring global and regional emission drivers to support the design of future low-carbon transition policies. As an important source of CO_2 emissions, the power sector is usually examined as a separate emission sector in previous global inventories [36–39], such as the Emissions Database for Global Atmospheric Research (EDGAR), the Community Emission Data System (CEDS), and the Carbon Dioxide Information Analysis Center (CDIAC). Given the difficulties in acquiring information on all power units, studies mainly use yearly country-level activity data and average emission factors to estimate emissions [40]. The Carbon Monitoring for Action (CARMA) database provides global plant-level CO_2 emissions data in 2009 and 2018 and has been widely utilized in environmental issues and policy making [41–44]. However, the CARMA database cannot provide time-series plant-level information, which limits the exploration of multi-scale emission trends and drivers. The first version of the Global Power Emission Database (GPED v1.0) includes global generating power plants that burn coal, oil, natural gas, biomass, or other fuels and tracks their CO_2 emissions as of 2010 [45]. Despite the remarkable progress made by existing databases, it is valuable to develop a long time-series global power plant database to provide uniform and consistent data supporting the analysis of global and regional drivers of power plant CO_2 emissions, as well as other scientific researches and the investigation of more innovative research topics.

To fill the gap in the development of time-series high-resolution power plant CO_2 emissions database and identification of global and regional driving forces in power unit structure and emissions, we first construct an extended version of Global Power plant Emissions Database (named GPED v1.1), which is based on the integration of different available global and regional power plant databases. In our previous work [40,46], we developed a unit-based coal-fired power plant database for China which is named China coal-fired Power Plant Emissions Database (CPED). CPED represents more accurate information for coal power units over China than other global databases [40], but it is not integrated in GPED because GPED is a publically available database while information in CPED is not publically available due to restriction from the original data owners. Instead, emissions in CPED were used to override GPED over China to support the analysis presented in this study. The combined database is in a significant position that can be used to comprehensively recognize global and regional driving forces of power plant CO_2 emissions over the last three decades. Specifically, we assess multi-scale spatial and temporal changes in generating capacities, fuel types, unit sizes, age structure and CO_2 emissions, as well as global and regional drivers of capacity evolution and CO_2 emission changes from 1990 to 2019. We identify five factors contributing to emissions changes: power generation demand, fossil fuel share, fuel mix, energy efficiency and emission intensity, and highlight the future best opportunities in climate mitigation for the power sector.

2 Method and data

2.1 Global Power plant Emissions Database version 1.1

2.1.1 Construction of the GPED v1.1

The new-built GPED v1.1 is developed on the basis of the extension of our previously developed GPED v1.0 [45], which encompasses more than 100,000 power units that burn coal, oil, natural gas, biomass, or other fuels operating during 1990-2019 worldwide. The basic information of power units, containing plant name, unit capacity, fuel type, starting year of operation, the year of decommissioning, and geophysical location, are completely derived in this database. The GPED v1.1 is developed by complying, combining, and harmonizing the available data related to power-generating units burning coal, natural gas, oil, biomass or other fuels. The diagram of the construction of the GPED v1.1 is presented in Fig. S1.

We begin by using multi versions of the WEPP databases [47] to compile unit-based information of generators in service and out of service during the period of 1990-2019, which provide information on the physical address, specific fuel type, installed capacity, status, starting year of operation, and retirement year of global power-generating units. Next, another database of Global Energy Monitor database (GEM) [48] is integrated to fill the missing unit information of physical address, installed capacity, status, and starting year of operation by mapping with the WEPP databases. Further, the GPED v1.1 combines and harmonizes the more comprehensive and reliable data contained in the national databases of the United States and India according to the data availability: the Emissions & Generation Resource Integrated Database (eGRID) for the United States [49] and the Indian Coal-fired Power Plants Database (ICPD) for India [50,51]. The eGRID is a comprehensive source of data from EPA's Clean Air Markets Division on the environmental characteristics of almost all electric power generated in the United States [49], including unit-level basic information and plant-level operation information (i.e. power generation) and CO_2 emissions for multi years. It is noted that unit-level operation and emission information based on the plant-level information from the eGRID only in the year of 2010 are carefully derived previously [45]. The ICPD only includes generator-level operation information for Indian coal-fired power units in the year of 2010 [50,51]. Under the comprehensive consideration of dataset consistency, unit-level information availability and integration difficulty among different datasets, available derived unit-level data in the year 2010 for both the United States and India are integrated during the development of the GPED v1.1 currently. In summary, the GPED v1.1 presents an integration of the best available unit-level data we think, which is developed on basis of various global and regional power plant database, including global datasets of the WEPP database and the GEM database, regional datasets covering main countries of the United States and India.

For the geographical locations of power plants, which are unavailable from the global WEPP dataset. We first obtain the exact latitudes and longitudes for the power plants existing in our database of previous version [45]. For the remaining plants with a total capacity >10 MW, we geolocate them by searching data from the GEM database and Google Earth. The locations of the remaining and smaller plants are collected by directly mapping the physical addresses contained in the WEPP database to Google Maps following our previous study [43].

2.1.2 Estimates of CO_2 emissions

Unit information related to the estimates of CO_2 emissions from above-mentioned global and regional datasets is also integrated. Where available, we directly adopt unit-based estimates of CO_2 emissions from existing databases (i.e. the eGRID in 2010). For other units contained in GPED v1.1, the estimates of CO_2 emissions depend on the activity rates and the CO_2 emission factor according to the following equation.

$$E_{i,m} = A_{i,j,m} \times EF_{s,k,m} \times 10^{-3} \quad (1)$$

where *k*, *i*, *j*, and *m* represent country, generating unit, fuel type, and year, respectively; *E* represents unit-based emissions (kg), *A* represents specific fuel consumption per unit (kg for solid- or liquid-fired units and m^3 for gas-fired units), and *EF* is the emission factor (g/kg for solid- or liquid-fired units and g/m^3 for gas-fired units).

Because detailed activity data (i.e. unit-level power generation and fuel consumption) for each generating unit are not available, we thus estimate unit-based activity data from country-level power generation and fuel consumption. Unit-level fuel consumption is a function of power generation and fuel consumption per unit power generation, and power generation is again determined by the installed capacity and annual operating hours. But of these, only installed capacity data are readily available, we therefore first estimate unit-level power generation from country-level power generation. Country-level power generation data from 1990-2018 are obtained from the International Energy Agency (IEA) [7] and extended to 2019 by using the BP Statistical Review of World Energy [52]. To estimate unit-level annual power generation, unit-level information of annual operating hours (i.e. capacity factor) is first collected from regional databases of the eGRID and ICPD, and we then apply to other years due to data availability [45]. For the rest of power units not contained in those regional databases, the annual operating hours of power units burning the same fuel (65 fuel types) are consistent at the country level according to the simplifying assumption of our previous study [45]. Therefore, we calculate unit-level power generation using equation (2).

$$G_{m,i,j} = G_{m,k,j} \times \frac{\lambda_m * C_i * T_i}{\sum \lambda_m C_{k,j} * T_{k,j}} \tag{2}$$

where *i*, *k*, *j*, and *m* represent the generating unit, country, fuel type, and year, respectively; *G* represents power generation; and λ represents the operating status according to the online year and retirement year of individual generating units. If the generator is operating, $\lambda = 1$; otherwise, $\lambda = 0$. *C* is the installed capacity of power units, and *T* is the annual operating hours.

Unit-level fuel consumption is further estimated starting from the country-level fuel consumption. As described above, country-level fuel consumption data from 1990-2018 are also derived from world energy statistics published by the IEA [7]. Based on energy consumption in 2018, we apply the growth rate from 2018-2019 by fuel type (coal, natural gas, and oil) and by country according to the BP Statistical Review of World Energy [52] to estimate 2019 energy consumption. Fuel consumption per unit power generated is inversely related to electric efficiency [43]. Instead, we directly adopt unit-based electric efficiency information from existing databases, which is applied for units for the whole period 1990-2019 as the electric efficiency is mainly related to electricity technology [45]. When detailed fuel consumption information (i.e. the electric efficiency) for remaining power units are not available from existing databases, we estimate electric efficiency by using the functions developed in our previous study [45] according to the nonlinear relationship between installed capacity and the electric efficiency of different fuel types. Here, therefore, unit-level activity rates where unavailable are finally estimated from country-level fuel consumption according to equation (3) below.

$$A_{m,i,j} = A_{m,k,j} \times \frac{\lambda_m \frac{C_i * T_i}{e_i}}{\sum \frac{\lambda_m C_{k,j} * T_{k,j}}{e_{k,j}}} \tag{3}$$

where *i*, *k*, *j*, and *m* represent the generating unit, country, fuel type, and year, respectively; *A* represents country-level fuel consumption (kg for solid- or liquid-fired units and m^3 for gas-fired units); and λ represents the operating status according to the online year and retirement year of individual generating units. If the generator is operating, $\lambda = 1$; otherwise, $\lambda = 0$. *C* is the installed capacity of power units, *T* is annual operating hours, and *e* is electric efficiency.

CO_2 emission factors are quantified according to guidelines from the Intergovernmental Panel on Climate Change (IPCC) [53] using equation (4).

$$EF_{CO_2,j,k,m} = CA \times O \times 44/12 \times H_{j,k,m} \tag{4}$$

where *j*, *k*, and *m* represent fuel type, country and operating year, respectively; EF_{CO_2} represents the CO_2 emission factor in g/kg; CA represents the carbon content in kg-C/GJ; O represents the carbon oxidation factor; $44/12$ is the molecular weight ratio of CO_2 to carbon; and H is the heating value in kJ/g for solid and liquid fuels and kJ/m^3 for gaseous fuels. In this study, the carbon oxidation factor is assumed to be 1, and carbon contents data are obtained from the IPCC guidelines [53]. The heat value of each fuel type and country is from the IEA [7].

In summary, CO_2 emissions and related information of technology, activity data, operation situation, emission factor employed in the emission estimates for each individual unit in the GPED v1.1 database covering the period of 1990-2019 are derived in various ways, which are again combined with the unit-level emissions information contained in the CPED to decompose and characterize global and regional drivers of CO_2 emissions.

2.2 CPED

The CPED includes detailed basic power plant information on the unit capacity, boiler type, operation and phasing-out procedures and geographical locations, as well as emission information on the activity data, operation situation, emission factors and CO_2 emissions of China's individual coal-fired units covering the whole period of 1990-2019 [40,46,54], which consists of more than 9,000 coal-fired electric-generating units. In detail, instead of modeling the related parameters of the activity rates, the annual coal use and power generation for each unit are directly available in the CPED, which can accurately reflect the differences of capacity factors and electric efficiencies among units. Again, annual CO_2 emission factors are estimated by using the national heating values of coal, which characterized the annual changes of coal quality. Unit-level CO_2 emissions are therefore estimated in a more accurate way. Unfortunately, information in CPED was not able to incorporated in to GPED due to the restriction of data sharing. The detailed unit-level information in CPED are then used to override information in GPED over China for this study, to represent the best knowledge of spatial and temporal evolutions of China's power unis and their emissions.

2.3 Uncertainty assessments

Uncertainty analysis is an important part of accuracy assessments of emissions inventories. Uncertainties in inventory can be caused by the incomplete information of fossil fuel consumption data, emission factors and other parameters. A comprehensive analysis of uncertainties in emissions is conducted at the national and unit levels using a Monte Carlo approach [55–57]. Monte Carlo simulations are employed to propagate the uncertainties induced by both fossil fuel consumption and emission factors to provide the uncertainty ranges for emission estimates. For uncertainties in national emissions, we first assume probability distributions for both fossil fuel consumption and emission factors. Then, random sampling of both the activity data and emission factors is conducted 10,000 times, generating 10,000 estimations of CO_2 emissions. The uncertainty range in this study is estimated by the lower and upper bounds of 95% confidential intervals around the central estimate of emissions [58]. The probability distributions and coefficients of variation (CVs, equal to one standard deviation divided by the mean) of the parameters are obtained from previous studies [36,39,40,45].

From the perspective of unit-level emission estimates, uncertainties associated with input parameters may vary over time and by country due to the different accuracies of information from global and national databases. Countries without available national databases could have higher uncertainties than countries with higher-quality data sources. Following the method used in our previous study [40,45], we randomly select one large coal-fired unit (≥300 MW) from nine key regions to demonstrate that the emission uncertainties differ among regions. The uncertainties can be considered larger for a coal power-generating unit operating in 1990 than for one operating in 2019 because the accuracy of unit-level information improved over time. We quantify the emission uncertainties of the selected coal power units for 1990 and 2019 to demonstrate the changes in uncertainties over time. We assume that both the unit-level energy consumption and emission factors follow a normal distribution with the CVs, as discussed above.

2.4 Decomposition of emission drivers

Decomposition analysis methods have been widely used to quantify the contribution of socioeconomic drivers to changes in environmental pressures [59–62]. The two most popular decomposition approaches are index decomposition analysis (IDA) and structural decomposition analysis (SDA). Compared to SDA, which is based on input-output tables [63,64], IDA is more suitable for time-series energy and emission studies [65,66]. Among IDA methodologies, the logarithmic mean Divisia index (LMDI) has been shown by past studies to be favorable because of its path independence, consistency in aggregation, and ability to handle zero values [67–69]. In this study, we choose LMDI to identify how each driving factor contributes to the changes in CO_2 emissions. The drivers are classified as power generation demand, fossil fuel share, fuel mix, generation efficiency and emission intensity, as shown in equation (5).

$$E = \sum_n^9 \sum_i^5 G_n \times \frac{Q_{n,i}}{G_n} \times \frac{G_{n,i}}{Q_{n,i}} \times \frac{A_{n,i}}{G_{n,i}} \times \frac{E_{n,i}}{A_{n,i}} \tag{5}$$

where *n* and *i* represent region and fuel type, respectively; nine regions are included in this study (see Fig. S2). Fuel type includes coal, oil, natural gas, biomass and others. *E* represents CO_2 emissions, *G* represents power generation, *Q* represents power generation from fossil fuels, and *A* represents energy consumption.

Hence, the arithmetic change in total emissions from year t+1 to year t (ΔE) is decomposed as follows:

$$\Delta E_n = E_n^{t+1} - E_n^t = \Delta G_n + \Delta S_n + \Delta M_n + \Delta I_n + \Delta T_n \tag{6}$$

$$\Delta G_n = \sum_i^5 \mathrm{L}(E_i^{t+1}, E_i^t) \ln\left(\frac{G^{t+1}}{G^t}\right) \tag{7}$$

$$\Delta S_n = \sum_i^5 \mathrm{L}(E_i^{t+1}, E_i^t) \ln\left(\frac{{Q_i}^{t+1}/G^{t+1}}{{Q_i}^t/G^t}\right) \tag{8}$$

$$\Delta M_n = \sum_i^5 \mathrm{L}(E_i^{t+1}, E_i^t) \ln\left(\frac{{G_i}^{t+1}/{Q_i}^{t+1}}{{G_i}^t/{Q_i}^t}\right) \tag{9}$$

$$\Delta I_n = \sum_i^5 \mathrm{L}(E_i^{t+1}, E_i^t) \ln\left(\frac{{A_i}^{t+1}/{G_i}^{t+1}}{{A_i}^t/{G_i}^t}\right) \tag{10}$$

$$\Delta T_n = \sum_i^5 \mathrm{L}(E_i^{t+1}, E_i^t) \ln\left(\frac{{E_i}^{t+1}/{A_i}^{t+1}}{{E_i}^t/{A_i}^t}\right) \tag{11}$$

$$\mathrm{L}(E_i^{t+1}, E_i^t) = (E_i^{t+1} - E_i^{t+1})/(\ln E_i^{t+1} - \ln E_i^t) \tag{12}$$

where *n* and *i* represent region and fuel type, respectively; $\mathrm{L}(E_i^{t+1}, E_i^t)$ is a weighting factor named the logarithmic mean weight; and ΔG is captured by the change in total power generation. The fossil fuel share effect (ΔS) measures the impact of changes in fossil fuel mix on power generation. The fuel mix effect (ΔM) measures the impact of changes in fuel mix on fossil fuel power generation. The generation efficiency effect (ΔI) represents the impact of changes in the thermal efficiency of fossil fuel power generation, and the emission factor effect (ΔT) captures the impact of changes in emission factors.

3. Results and discussion

3.1 Evolution of technologies

The capacity of global fossil fuel and biomass-fired power plants experienced a substantial increase during the past three decades. Figure 1 displays the capacity trends and geographic distribution evolutions of global power plants during 1990-2019. Driven by the continuous growth of global power generation demand, the capacity of global fossil fuel-fired and biomass-fired power plants was 2.3 times higher in 2019 than in

1990. The global total capacity increased from 1,774 GW in 1990 to 4,139 GW in 2019, with an average expansion rate of 3.0% per year (Fig. S3). The capacity expansion of fossil fuel-fired and biomass-fired power plants was more rapid in developing countries than in developed countries. Here, we take China and the United States as examples; the former had a 10.3-fold increase in capacities of fossil fuel-fired and biomass-fired power plants while the latter had a 0.5-fold increase from 1990 to 2019. In addition, the expansion of power infrastructures has accelerated in India but decelerated in the United States and Europe since 2010.

Coal-fired power plants comprise the majority of global fossil fuel-fired power plants, accounting for 49.0% of the total capacity of all biomass- and fossil fuel-fired power plants in 2019 (Fig. S4). The contributions of gas-fired and oil-fired plants were 38.0% and 10.6%, respectively. However, the capacity growth rate (4.3%) of global natural gas power plants was higher than that (2.8%) of global coal power plants over the past few decades (Fig. S5), representing progress in the shift from coal to natural gas power. A decline in the number of coal-fired power plants and the rapid growth of natural gas power plants can be observed in the United States and Western Europe over the past three decades. In contrast, many large coal-fired power plants were constructed in the northern and eastern coastal regions of China, where large coal mines are located. Similarly, in India, the number of coal-fired power plants increased dramatically during these three decades, mainly located near coal mines and in coastal regions. As a result of the new construction of large coal power units (≥600 MW), the contributions of these units in China and India increased significantly, from 1.4% to 47.2% and 0.0% to 35.4% of the total capacity of coal power units during 1990-2019, respectively (Fig. S6).

The turnover and development of power generating capacity supports the application of large and more advanced electricity technologies, and the thermal efficiency of global fossil fuel-fired power plants greatly improved over the past three decades. Figure 2 presents the changes of global power fleet structure by thermal efficiency (indicating by consumption rate), size and fuel type from 1990 to 2019. For power plants with consumption rates greater than 400 gce kWh^{-1}, their contributions to the total number of all power plants declined from 61% to 17% during 1990-2019. For power units with the same fuel type, large units had lower energy consumption intensity because of the use of more advanced combustion technology. Fig. 2b shows that the capacity share of large units (≥300 MW) increased from 62% in 1990 to 65% in 2019, whereas the share of small units (<100 MW) dropped to 20% during that period. In particular, the construction of large units (≥600 MW) has accelerated since 2005, and their capacity increased from 146 GW in 2005 to 262 GW in 2019 due to policies to encourage larger coal power units in China. Fig. 2c further illustrates the measures taken worldwide to support the transition to large power units during the expansion of power units. The share of large units (≥100 MW) increased significantly, from 5% to 45% of the number of all newly built units from 1990 to 2019, respectively, whereas the share of small units (<10 MW) decreased from 75% to 25% in the same period. The average capacity of newly built power units in 2019 was 40 MW, 3 times the value in 1990 (13 MW). With regard to the switch in fuel mix, the share of natural gas power plants increased significantly, from 26.9% to 40.5% of the total capacity of global fossil fuel-fired power plants, whereas the contribution of oil power plants decreased from 20% to 5%.

3.2 CO_2 emission trends

Here, we conduct a multi-scale analysis of the changes in the characteristics of CO_2 emissions for global power plants. Section 3.2.1 presents global and regional CO_2 emission trends. Sections 3.2.2 and 3.2.3 present the evolutions of age-based CO_2 emissions, and identify those low-efficiency units based on unit-level quantification, respectively.

3.2.1 Interannual emissions

Figure 3 shows the trends of the CO_2 emissions of global power plants by region and by fuel type from 1990 to 2019 estimated in this study. Driven by the expansion of power infrastructures and the increase in the demand for power generation, the CO_2 emissions of global fossil fuel- and biomass-fired power plants increased continuously from 7.5 Gt in 1990 to 13.9 Gt in 2019, with a 2.2% growth rate per year. The CO_2 emissions of global fossil fuel-fired power plants increased every decade. The average growth rate was 182 Mt yr−1 in the 1990s, accelerated to 330 Mt yr−1 in the 2000s, and finally returned to 143 Mt yr−1 in the 2010s due to the slowing of power plants expansion. Notably, the CO_2 emissions of global power plants were -1.7% in 2018-2019. The continued declines in CO_2 emissions of coal-fired power plants in the United States and Europe, as well as the slowdown in coal power growth in China and India (Fig. S7), resulted in this modest decline in the CO_2 emissions of global power plants.

In the United States and Europe, the CO_2 emissions of power plants peaked and showed a continued decline, whereas the CO_2 emissions of China, India and the rest of the world increased steadily. The major emitters shifted from developed countries (the United States and Europe) to developing countries (China and India) over the past 30 years. The United States and Europe accounted for 29.3% and 27% of the total emissions of global power plants in 1990, whereas China and India accounted for 48.6% and 20% of the total emissions of global power plants in 2019, respectively. From the perspective of fuel type, the CO_2 emission trends in global power plants were mainly dominated by coal-fired power plants, followed by natural gas-fired power plants and oil-fired power plants. Coal-fired power plants accounted for 69.1% and 69.8% of the global CO_2 emissions of power plants in 1990 and 2019, respectively. The growth rate of CO_2 emissions of natural gas-fired power plants was the largest at 3.6% per year during 1990-2019. In contrast, the CO_2 emissions of oil-fired power plants show a declining trend with a growth rate of -2.0% at the same period.

3.2.2 Age-based emission evolutions of power units

Figure 4 shows the age-based evolution of global CO_2 emissions by coal versus natural gas and oil from 1990 to 2019 (1990 in Fig. 4a, 2000 in Fig. 4b, 2010 in Fig. 4c and 2019 in Fig. 4d), which indicates the differential power generation demand and associated power unit development among regions. Globally, the average age of fossil fuel-fired power units showed an increasing trend in 1990-2019, for a 1% growth rate per year (Fig. S8a). With the rapid growth in the power generation demand, China, India and other developing countries built a large amount of coal power units and the age structure of coal power units was pretty young. In contrast, coal power unit fleets operating in the United States and Europe continuously grew older, averaging 41 and 36 years old in 2019 (Fig. S8b). The aging of coal power plant fleet in the United States and Europe was determined by the relatively stable power generation demand and the fuel switching from coal to natural gas, and that’s why we see the carbon peak before 2005 in these regions.

Young power units represent future commitment and pose huge challenges to the deep decarbonization of the power system. With the dramatic increase in the power generation demand, young power units (<12 years) continuously played important roles in the contributions of global CO_2 emissions, accounting for 38.5%, 29.7%, 39.7% and 39.9% of the total CO_2 emissions in 1990, 2000, 2010 and 2019, respectively. While the regional contributions in CO_2 emissions from young power units have significantly changed over times. For example, coal power units with age <12 year in the United States and Europe in 1990 determined the characteristics of CO_2 emission distributions, strikingly contributing 49% of global emissions from all young coal power. With new-built coal-fired capacity almost disappearing in the United States and Europe, the development of coal power in China, India and the rest of Asia dominates almost all of CO_2 emissions from young coal power units by 2019 (91%), which also indicates the drivers of global emission changes are the results of different and mixed regional emission drivers at the different developmental stages. Specially, China contributed the largest share (55.4%) of emissions from all young coal power units in 2019, followed by India (24.5%). In comparison, 33.3% and 21.4% of emissions from all young gas and oil power units were from the Middle East and North Africa and the rest of Asia, respectively. From the perspective of new-built unit in the most recent years, CO_2 emissions from the youngest coal power units (<3 years) decreased 63.6% between 2010 and 2019 (from 1.1 Gt in 2010 to 0.4 Gt in 2019), which is explained by the slowed expansion of coal power units in China and India. In contrast, the aging power plant fleet represents a critical opportunity in the transition to cost-effective and low-carbon power systems. Globally, the CO_2 emissions of old power units (>41 years old) increased from 68 Mt in 1990 to 1,732 Mt in 2019, with the share increasing from 1.0% to 13.2% of total emissions in 1990 and 2019, respectively. Particularly, the United States and Europe accounted for 48.8% and 23.2% of emissions from global old coal power units in 2019, respectively, which is associated with the aged structure of coal power units.

3.2.3 Low-efficiency power units

High-resolution emission information can help us identify the detailed evolutions for each unit. Figure 5 shows the relationship between power generation and annual CO_2 emissions from coal-fired units in China, India, Europe and the United States, highlighting the evolutions of low-efficiency units between 1990 and 2019, which we define as those units whose emission intensity (i.e. tons CO_2 per MWh) is more than 90th percentile greater than the average emission intensity in 1990 in the same region. Across all regions, a large fraction of total CO_2 emissions was produced by a disproportionately small fraction of total power generation. For instance, 4.3% and 0.6% of total power generation from coal-fired units in the United States and Europe produced 6.7% and 2.1% of total CO_2 emissions in 1990 and 2019, respectively.

Driven by the large-scale and continuous construction of new units, which tend to have higher operating efficiencies, a decrease in the share of the power generation of low-efficiency coal power units was observed in all regions from 1990 to 2019. For example, with 13.2% thermal efficiency improvement, the share of low-efficiency coal power capacity decreased from 4.6% to 0.6% in Europe from 1990-2019. However, the evolution of low-efficiency coal power units had different characteristics among different regions. The number of low-efficiency coal power units in China and India increased from 63 units to 195 units (from 904 MW to 3,287 MW) and from 40 units to 104 units (from 2,540 MW to 4,703 MW) during 1990-2019, respectively. A slight increase of unit number is mainly because the rapid expansion of units from less than a megawatt to more than a gigawatt, whose efficiencies significantly varied. In contrast, with the retirement of aged and low-efficiency units, low-efficiency coal power units from the United States and Europe decreased from 132 to 82 (from 1,230 MW to 701 MW) and from 160 units to 41 units (from 3,540 MW to 403 MW) in the same period, respectively. The average age of those low-efficiency coal units was 19 and 23 years for China and India compared with 45 and 43 years for the United States and Europe, respectively. Additionally, although a smaller number of units are recognized as the low-efficiency ones within each region, the value of mean emission intensities further reveal the large disparities among different regions. By 2019, 1,395 gCO_2/kwh of mean emission intensity in India is much higher than 1,001 gCO_2/kwh of that in the United States. These low-efficiency coal power units in different regions, especially for units in the developing regions, reveal targeted opportunities by optimizing the power fleet in mitigating CO_2 emissions.

3.3 Drivers of CO_2 emissions

The characteristics of age-based CO_2 emission distributions and unit-level emission intensities had revealed the different driving forces in changes of CO_2 emission trends at the global and regional scale to some extent, and we further conducted a systematical decomposition of global and regional drivers. Figure 6 shows the effects of power generation demand, energy efficiency, fuel mix and fossil fuel share on CO_2 emissions during 1990-2019, as well as the regional contribution to the changes in the emissions. Overall, global CO_2 emissions grew by 6.4 Gt between 1990 and 2019, and the 85.8% increase in CO_2 emissions was dominated by strong power generation demand growth, which is also verified by the age structure of CO_2 emissions from global power units in Fig. 4. In the absence of other factors, power generation demand growth would have caused emissions to increase by 31.3% and 44.3% during the 1990-2000 and 2000–2010 periods, respectively, and it drove the relatively slower increase of 26.3% in 2010–2019. In comparison, improvements in the efficiency of power generation were the main drivers of decreasing global CO_2 emissions in 1990-2019 (accounting for 53.6% of the decrease in CO_2 emissions), followed by the fuel mix effect (37.0%) and the fossil fuel share effect (9.4%). The decreasing share of the low-efficiency power units shown in Fig. 5 also indicates the improvements in the efficiency of power generation. Independent of other factors, improvements in the efficiency of power generation caused emissions to decrease by 7.6%, 5.6% and 5.6% during the 1990-2000, 2000–2010 and 2010–2019 periods, respectively. Changes in the drivers of global emissions among different periods were associated with regional economic growth, environmental policy and technological advances. For example, the global fossil fuel share decreased dramatically with the rapid growth in renewable power generation. The decrease in the global fossil fuel share reflects the role change of driving forces from 2010–2019, with a more significant and positive impact on global CO_2 emission reductions in comparison with other periods. Specifically, the fossil fuel share drove the emissions decline of 8.7% from 2010-2019, whereas it increased emissions by 3.9% and 5.2% during the 1990–2000 and 2000–2010 periods, respectively.

We further compare the regional drivers of power plant CO_2 emissions in the 1990-2000 (Fig. 6b), 2000-2010 (Fig. 6c) and 2010-2019 (Fig. 6d) periods. Developing countries were major contributors to emissions increases, driven by the growth of power generation demand; in particular, China and India accounted for 142% and 54% of total emission increases in the 2010-2019 period, respectively. Additionally, the improvements of energy efficiency played a similar role in emission reductions in both developed and developing countries across all the periods. Particularly, improvements of energy efficiencies for power units in China, the Middle East and North Africa, and India also contributed 34%, 7% and 6% of global CO_2 emission reductions in 2010-2019, respectively, which is explained by the large-scale construction of more advanced units and the decrease of mean emission intensities in developing countries in recent years (Fig. 6). In contrast, global emissions changes driven by the fossil fuel mix (i.e. the relative shares of coal, oil and natural gas) were largely dominated by the United States (63.7%) and Europe (31.6%) in 1990-2019, which was benefited by the coal to natural gas switching in the developed regions since the early stage (Fig. 4). Independent of other factors, fuel mix changes in the United States and Europe together decreased global emissions by 6.7% (622 Mt) during 2000-2010. Another important driving force in decreasing emissions, especially during 2010-2019, was the decrease of fossil fuel share, whose effect on emission reductions was primarily driven by the United States, China, Europe and India during that period (accounting for 38%, 25%, 22% and 11% of total emission reductions from the decrease of fossil fuel share during 2010-2019, respectively). Finally, the combined effects of these four drivers resulted in the global increase of CO_2 emissions, which were almost dominated by China, India and the rest of Asia during 1990-2019 (totally accounting for 96% of total emission changes), while Europe and the United States made an important contribution to decreasing emissions at the same period. More importantly, when comparing the growth rate of power generation demand and the increase rate of CO_2 emissions among different stages in China, India and the rest of Asia, we find that the growth rate of power generation demand is pretty close to the increase rate of CO_2 emissions before 2010. While during 2010-2019, CO_2 emissions only increased by 82% in China in contrast to 142% of the power generation increase. It is indicated the increasingly important contributions of the improvements of energy efficiencies, fuel mix and the decrease of fossil fuel share, which again confirmed the effectiveness of China's clean air actions. In summary, the comprehensive analysis of global and regional drivers in CO_2 emissions can help future design of power plant polices on fleet optimizations and carbon emission reductions.

3.4 Uncertainty and comparison

Uncertainty both at the country and unit level is quantified in this study. The gray area in Fig. S9 indicates the 95% confidential interval of global CO_2 emission estimations in this study. The average uncertainty of emissions from global power plants in 2019 is estimated to be -20.5% to 22.1%. The higher uncertainty range of the emission estimates is dominated by the uncertainties in the activities of facilities. The development of a local database of the actual activities of individual units helps to reduce the uncertainties. The uncertainty ranges of CO_2 emission estimates narrow gradually and decline from -28.8%–31.9% in 1990 to -16.4%–17.3% in 2019 (Fig. S9), representing more and more improved knowledge of the underlying data over time. Many of the input data in the GPED in 1990 were determined by extrapolations and assumptions associated with high uncertainties, whereas the uncertainty ranges for the 2019 emission estimates are significantly reduced because of the extensive use of unit-specific data. In addition, a better understanding of activities for each unit in 2019 is the primary reason for the narrowed uncertainties in CO_2 emission estimates.

We further demonstrate the variation in emission uncertainties over time at the unit level. There was larger uncertainty in the selected coal power units (≥300 MW) in 1990 than in 2019. For example, the CO_2 emission uncertainty from the coal power units (≥300 MW) in China was -22.5%–24.0% in 1990 and -11.4%-11.9% in 2019. The uncertainty ranges for the 2019 estimates were significantly reduced compared with those for the 1990 estimates because more unit-specific information became available in 2019, which is consistent with the trends of global uncertainty ranges. Coal power units in China, India and the United States had smaller uncertainty ranges than those in Europe due to the availability of unit-level data (e.g., -11.4%–11.9% for the selected coal power unit (≥300 MW) in China compared to -22.5%–24.2% in Europe). The unit-level uncertainty ranges in China, India and the United States were smaller than the global average uncertainty ranges due to the application of regional databases, whereas other regions corresponded to higher uncertainties because some key parameters (e.g., activities and efficiency) were derived from extrapolations and assumptions.

In addition to the uncertainties of fossil fuel consumption and emission factors considered in the Monte Carlo techniques described above, the emission inventory when using the datasets included other uncertainties, such as the completeness of the datasets and the accuracy of the elementary information the datasets, which were difficult to quantify. First, with respect to the completeness of the datasets, despite the great effort to compile a complete dataset of global power plants, the GPED database might still lack some power-generating units due to the tremendous information required to be comprised worldwide. Second, in terms of the accuracy of the elementary information in the dataset, accurately depicting the elementary information of power-generating units and tracking their evolution are the basis of the development of high-resolution emission databases. Taking capacity as an example, the capacity of a specific power-generating unit could impact CO_2 emission estimates by affecting the estimates of energy consumption at the unit level in this study, which had little effect on total emissions but increased the uncertainty in unit-level emissions.

We finally compare our new emissions database with other bottom-up emission inventories, as shown in Fig. S9, in which multi-year estimates are provided. The discussion is focused on inventories that are widely used in the community, i.e., EDGAR version 5.1 and CEDS. We compare the CO_2 emission estimates of the different emission inventories. Our estimates are comparable with those of EDGAR and CEDS, which are more consistent with EDGAR and are approximately 1.8%–6.6% higher than CEDS. The difference between our results and other emission inventories is possibly associated with the discrepancy in the estimates of activity rates and emission factors. Take China as an example, detailed unit-level activity data are obtained from China's Ministry of Environmental Protection in this study, whereas the activity data of the power sector are directly collected from the IEA in other studies.

4. Conclusion and discussion

The capacity of global fossil-fuel- and biomass-fired power plants experienced a substantial increase, driven by the growing demand for power generation during the past three decades. CO_2 emissions increased from 7.5 Gt in 1990 to 13.9 Gt in 2019 at a 2.2% growth rate per year, mainly dominated by the development of coal-fired power capacity in developing countries. In the most of developed regions, such as United States and Europe, CO_2 emissions from the power sector peaked before 2005, benefiting from the improvement in energy efficiency and fuel switching from coal to natural gas in the context of relatively stable power demand. In contrast, trends of ever-growing CO_2 emissions and power demand in developing countries were observed and are expected to continue to climb to a new peak although the effectiveness of the fossil fuel share decrease and energy efficiency improvement was confirmed. Additionally, there are substantial gaps in CO_2 emission intensities of the developing regions compared with the developed regions. Economies with higher CO_2 emission intensities from power plants should enhance the energy efficiencies of fossil fuel-fired power plants by using more advanced electricity technologies and accelerate the transitions of emission-free renewable energy (e.g., solar and wind) in the context of carbon neutrality worldwide, aiming to develop low-carbon power systems in the future for climate change mitigation.

Our database could add important insights to policy-relevant discussions of climate change mitigation for the global power plants. Currently, the power sector is the top CO_2 emitter among various sectors and has great significance for achieving climate targets and net-zero emissions. In the context of the Paris Agreement, the emissions of power plants should be continuously monitored and quantified to evaluate the effectiveness of climate-action efforts in reducing future carbon emissions. For developed countries, fuel switching from coal to natural gas helps to achieve short-term emission reductions [33–35]. However, for the long-term future, in most scenarios, accomplishing a global transition to energy systems with net-zero emissions may require a large share of renewable electricity (i.e., solar and wind resources) [70–72]. Developing countries could switch directly from coal power to renewables rather than using natural gas or other fossil fuel given the rapid decrease in renewable electricity costs and the pressure of rapid transitions [73–75]. The expansion of renewables will thus likely represent an increasingly significant factor driving future emission reductions in the power sector, which could be captured and evaluated using our data-driven assessment in future. In summary, our combined databases could further contribute to applications related to climate change mitigation, facilitate multiple research perspectives for global environmental issues and policy making, and enhance our abilities to track emission mitigation progress toward sustainable power systems and support effective strategies for future emission mitigation.

Data availability

For the company name, plant name, plant location, number of power generating units, CO_2 emissions at the unit-level contained in the GPED is available at: http://gidmodel.org.cn/dataset-gped. Other information at unit-level is obtained from commercial database and not publically available. For the database CPED, unit-level information is not publically available due to restriction from data providers.

Acknowledgements

This work was supported by the National Natural Science Foundation of China (41921005 and 91744310).

References

[1] Matthews HD, Caldeira K. Stabilizing climate requires near-zero emissions 2008;35. https://doi.org/10.1029/2007GL032388.

[2] Allen MR, Frame DJ, Huntingford C, Jones CD, Lowe JA, Meinshausen M, et al. Warming caused by cumulative carbon emissions towards the trillionth tonne. Nature 2009;458:1163–6. https://doi.org/10.1038/nature08019.

[3] Zickfeld K, Eby M, Matthews HD, Weaver AJ. Setting cumulative emissions targets to reduce the risk of dangerous climate change. PNAS 2009;106:16129–34.

[4] Goh T, Ang BW, Su B, Wang H. Drivers of stagnating global carbon intensity of electricity and the way forward. Energy Policy 2018;113:149–56. https://doi.org/https://doi.org/10.1016/j.enpol.2017.10.058.

[5] International Energy Agency. CO_2 Emissions from Fuel Combustion 2018 2018. https://doi.org/10.1787/co2_fuel-2018-en.

[6] Tong D, Zhang Q, Zheng Y, Caldeira K, Shearer C, Hong C, et al. Committed emissions from existing energy infrastructure jeopardize 1.5 °C climate target. Nature 2019;572:373–7. https://doi.org/10.1038/s41586-019-1364-3.

[7] International Energy Agency. Key World Energy Statistics 2020. Stat Rep 2020;33:4649.

[8] Jiang J, Ye B, Liu J. Research on the peak of CO2 emissions in the developing world: Current progress and future prospect. Appl Energy 2019;235:186–203. https://doi.org/10.1016/j.apenergy.2018.10.089.

[9] Chen ST, Kuo HI, Chen CC. The relationship between GDP and electricity consumption in 10 Asian countries. Energy Policy 2007;35:2611–21. https://doi.org/10.1016/j.enpol.2006.10.001.

[10] Chen J, Wang P, Cui L, Huang S, Song M. Decomposition and decoupling analysis of CO_2 emissions in OECD. Appl Energy 2018;231:937–50. https://doi.org/10.1016/j.apenergy.2018.09.179.

[11] Zhao W, Cao Y, Miao B, Wang K, Wei YM. Impacts of shifting China's final energy consumption to electricity on CO_2 emission reduction. Energy Econ 2018;71:359–69. https://doi.org/10.1016/j.eneco.2018.03.004.

[12] Williams JH, DeBenedictis A, Ghanadan R, Mahone A, Moore J, Morrow WR, et al. The technology path to deep greenhouse gas emissions cuts by 2050: The pivotal role of electricity. Science (80-) 2012;335:53–9. https://doi.org/10.1126/science.1208365.

[13] Knobloch F, Hanssen S V., Lam A, Pollitt H, Salas P, Chewpreecha U, et al. Net emission reductions from electric cars and heat pumps in 59 world regions over time. Nat Sustain 2020;3:437–47. https://doi.org/10.1038/s41893-020-0488-7.

[14] Qin Y, Höglund-Isaksson L, Byers E, Feng K, Wagner F, Peng W, et al. Air quality–carbon–water synergies and trade-offs in China's natural gas industry. Nat Sustain 2018;1:505–11. https://doi.org/10.1038/s41893-018-0136-7.

[15] Tong D, Cheng J, Liu Y, Yu S, Yan L, Hong C, et al. Dynamic projection of anthropogenic emissions in China: methodology and 2015–2050 emission pathways under a range of socio-

economic, climate policy, and pollution control scenarios. Atmos Chem Phys 2020;20:5729–57. https://doi.org/10.5194/acp-2019-1125.

[16] Pfeiffer A, Millar R, Hepburn C, Beinhocker E. The ‘2°C capital stock’ for electricity generation: Committed cumulative carbon emissions from the electricity generation sector and the transition to a green economy. Appl Energy 2016;179:1395–408. https://doi.org/10.1016/j.apenergy.2016.02.093.

[17] Fofrich R, Tong D, Calvin K, Boer HS De, Emmerling J, Fricko O, et al. Early retirement of power plants in climate mitigation scenarios OPEN ACCESS Early retirement of power plants in climate mitigation scenarios 2020.

[18] Li L, Shan Y, Lei Y, Wu S, Yu X, Lin X, et al. Decoupling of economic growth and emissions in China’s cities: A case study of the Central Plains urban agglomeration. Appl Energy 2019;244:36–45. https://doi.org/10.1016/j.apenergy.2019.03.192.

[19] Pour N, Webley PA, Cook PJ. Opportunities for application of BECCS in the Australian power sector. Appl Energy 2018;224:615–35. https://doi.org/10.1016/j.apenergy.2018.04.117.

[20] Hein KRG, Bemtgen JM. EU clean coal technology-Co-combustion of coal and biomass. Fuel Process Technol 1998;54:159–69. https://doi.org/10.1016/S0378-3820(97)00067-2.

[21] Khanna N, Fridley D, Zhou N, Karali N, Zhang J, Feng W. Energy and CO_2 implications of decarbonization strategies for China beyond efficiency: Modeling 2050 maximum renewable resources and accelerated electrification impacts. Appl Energy 2019;242:12–26. https://doi.org/10.1016/j.apenergy.2019.03.116.

[22] Thakur T, Deshmukh SG, Kaushik SC, Kulshrestha M. Impact assessment of the Electricity Act 2003 on the Indian power sector. Energy Policy 2005;33:1187–98. https://doi.org/10.1016/j.enpol.2003.11.016.

[23] Rowlands IH. The European directive on renewable electricity: Conflicts and compromises. Energy Policy 2005;33:965–74. https://doi.org/10.1016/j.enpol.2003.10.019.

[24] Lehmann P, Creutzig F, Ehlers MH, Friedrichsen N, Heuson C, Hirth L, et al. Carbon lock-out: Advancing renewable energy policy in Europe. Energies 2012;5:323–54. https://doi.org/10.3390/en5020323.

[25] del Río P, Hernández F, Gual M. The implications of the Kyoto project mechanisms for the deployment of renewable electricity in Europe. Energy Policy 2005;33:2010–22. https://doi.org/10.1016/j.enpol.2004.03.022.

[26] Meckling J, Allan BB. The evolution of ideas in global climate policy. Nat Clim Chang 2020. https://doi.org/10.1038/s41558-020-0739-7.

[27] Martin G, Saikawa E. Effectiveness of state climate and energy policies in reducing power-sector CO2 emissions. Nat Clim Chang 2017;7:912–9. https://doi.org/10.1038/s41558-017-0001-0.

[28] Springer C, Evans S, Lin J, Roland-Holst D. Low carbon growth in China: The role of emissions trading in a transitioning economy. Appl Energy 2019;235:1118–25. https://doi.org/10.1016/j.apenergy.2018.11.046.

[29] Steckel JC, Hilaire J, Jakob M, Edenhofer O. Coal and carbonization in sub-Saharan Africa. Nat Clim Chang 2020;10:83–8. https://doi.org/10.1038/s41558-019-0649-8.

[30] Ang BW, Goh T. Carbon intensity of electricity in ASEAN: Drivers, performance and outlook. Energy Policy 2016;98:170–9. https://doi.org/10.1016/j.enpol.2016.08.027.

[31] Dong J, Xue G, Dong M, Xu X. Energy-saving power generation dispatching in China: Regulations, pilot projects and policy recommendations - A review. Renew Sustain Energy Rev 2015;43:1285–300. https://doi.org/10.1016/j.rser.2014.11.037.

[32] Maruyama N, Eckelman MJ. Long-term trends of electric efficiencies in electricity generation in developing countries. Energy Policy 2009;37:1678–86. https://doi.org/10.1016/j.enpol.2008.12.004.

[33] Wilson IAG, Staffell I. Rapid fuel switching from coal to natural gas through effective carbon pricing. Nat Energy 2018;3:365–72. https://doi.org/10.1038/s41560-018-0109-0.

[34] Pettersson F, Söderholm P, Lundmark R. Fuel switching and climate and energy policies in the European power generation sector : A generalized Leontief model. Energy Econ 2012;34:1064–73. https://doi.org/10.1016/j.eneco.2011.09.001.

[35] Feng K, Davis SJ, Sun L, Hubacek K. Drivers of the US CO_2 emissions 1997-2013. Nat Commun 2015;6:1–8. https://doi.org/10.1038/ncomms8714.

[36] Janssens-Maenhout G, Crippa M, Guizzardi D, Muntean M, Schaaf E, Dentener F, et al. EDGAR v4.3.2 Global Atlas of the three major Greenhouse Gas Emissions for the period 1970 - 2012. Earth Syst Sci Data 2019;11:959–1002. https://doi.org/10.5194/essd-2018-164.

[37] Hoesly RM, Smith SJ, Feng L, Klimont Z, Janssens-Maenhout G, Pitkanen T, et al. Historical (1750-2014) anthropogenic emissions of reactive gases and aerosols from the Community Emissions Data System (CEDS). Geosci Model Dev 2018;11:369–408. https://doi.org/10.5194/gmd-11-369-2018.

[38] Oda T, Maksyutov S, Andres RJ. The Open-source Data Inventory for Anthropogenic CO_2, version 2016 (ODIAC2016): A global monthly fossil fuel CO_2 gridded emissions data product for tracer transport simulations and surface flux inversions. Earth Syst Sci Data 2018;10:87–107. https://doi.org/10.5194/essd-10-87-2018.

[39] Janssens-Maenhout G, Crippa M, Guizzardi D, Dentener F, Muntean M, Pouliot G, et al. HTAP-v2.2: A mosaic of regional and global emission grid maps for 2008 and 2010 to study hemispheric transport of air pollution. Atmos Chem Phys 2015;15:11411–32. https://doi.org/10.5194/acp-15-11411-2015.

[40] Liu F, Zhang Q, Tong D, Zheng B, Li M, Huo H, et al. High-resolution inventory of technologies, activities, and emissions of coal-fired power plants in China from 1990 to 2010. Atmos Chem Phys 2015;15:13299–317. https://doi.org/10.5194/acp-15-13299-2015.

[41] Ummel K. Carma Revisited: An Updated Database of Carbon Dioxide Emissions from Power Plants Worldwide. Ssrn 2013. https://doi.org/10.2139/ssrn.2226505.

[42] Wheeler D, Ummel K. Calculating Carma: Global Estimation of CO_2 Emissions from the Power Sector. Ssrn 2008. https://doi.org/10.2139/ssrn.1138690.

[43] Apriliani IM, Purba NP, Dewanti LP, Herawati H, Faizal I. Reducing CO_2 emissions by targeting the world's hyper-polluting power plants. Environ Res Lett 2021;2:56–61.

[44] Research highlights. Target the super polluters for big climate benefits. Nature 2021;595.

[45] Tong D, Zhang Q, Davis SJ, Liu F, Zheng B, Geng G, et al. Targeted emission reductions from global super-polluting power plant units. Nat Sustain 2018;1:59–68. https://doi.org/10.1038/s41893-017-0003-y.

[46] Tong D, Zhang Q, Liu F, Geng G, Zheng Y, Xue T, et al. Current Emissions and Future Mitigation Pathways of Coal-Fired Power Plants in China from 2010 to 2030. Environ Sci Technol 2018;52:12905–14. https://doi.org/10.1021/acs.est.8b02919.

[47] Platts SG. World Electric Power Plant Database (WEPP) 2020.

[48] Global Energy Monitor 2020.

[49] (USEPA) UEPA. Emissions & Generation Resource Integrated Databasee (eGRID). https://doi.org/https://www.epa.gov/energy/egrid.

[50] Lu Z, Streets DG, De Foy B, Krotkov NA. Ozone monitoring instrument observations of interannual increases in SO2 emissions from Indian coal-fired power plants during 2005-2012. Environ Sci Technol 2013;47:13993–4000. https://doi.org/10.1021/es4039648.

[51] Lu Z, Streets DG. Increase in NOx emissions from Indian Thermal Power Plants during 1996-2010: Unit-based inventories and Multisatelite observations. Environ Sci Technol 2012;46:7463–70. https://doi.org/dx.doi.org/10.102/es300831.

[52] BP Statistical Review of World Energy. Ed BP Stat Rev World Energy 2019:1–69.

[53] Guidelines I, Greenhouse N, Inventories G. 2006 IPCC Guidelines for National Greenhouse Gas Inventories. IPCC 2006.

[54] Wu R, Liu F, Tong D, Zheng Y, Lei Y, Hong C, et al. Air quality and health benefits of China's emission control policies on coal-fired power plants during 2005-2020.

[55] Liu Z, Guan D, Wei W, Davis SJ, Ciais P, Bai J, et al. Reduced carbon emission estimates from fossil fuel combustion and cement production in China. Nature 2015;524:335–8. https://doi.org/10.1038/nature14677.

[56] Zhao Y, Zhou Y, Qiu L, Zhang J. Quantifying the uncertainties of China's emission inventory for industrial sources: From national to provincial and city scales. Atmos Environ 2017;165:207–21. https://doi.org/10.1016/j.atmosenv.2017.06.045.

[57] Li M, Zhang Q, Kurokawa JI, Woo JH, He K, Lu Z, et al. MIX: A mosaic Asian anthropogenic emission inventory under the international collaboration framework of the MICS-Asia and HTAP. Atmos Chem Phys 2017;17:935–63. https://doi.org/10.5194/acp-17-935-2017.

[58] Peng L, Zhang Q, Yao Z, Mauzerall DL, Kang S, Du Z, et al. Underreported coal in statistics: A survey-based solid fuel consumption and emission inventory for the rural residential sector in China. Appl Energy 2019;235:1169–82. https://doi.org/10.1016/j.apenergy.2018.11.043.

[59] Hong C, Burney JA, Pongratz J, Nabel JEMS, Mueller ND, Jackson RB, et al. Global and regional drivers of land-use emissions in 1961–2017. Nature 2021;589. https://doi.org/10.1038/s41586-020-03138-y.

[60] Xu S, Zhang W, Li Q, Zhao B. Decomposition Analysis of the Factors that Influence Energy Related Air Pollutant Emission Changes in China Using the SDA Method. https://doi.org/10.3390/su9101742.

[61] Liu N, Ma Z, Kang J. A regional analysis of carbon intensities of electricity generation in China. Energy Econ 2017;67:268–77. https://doi.org/10.1016/j.eneco.2017.08.018.

[62] De Oliveira-De Jesus PM. Effect of generation capacity factors on carbon emission intensity of electricity of Latin America & the Caribbean, a temporal IDA-LMDI analysis. Renew Sustain Energy Rev 2019;101:516–26. https://doi.org/10.1016/j.rser.2018.11.030.

[63] Guan D, Meng J, Reiner DM, Zhang N, Shan Y, Mi Z, et al. Structural decline in China's CO_2 emissions through transitions in industry and energy systems. Nat Geosci 2018;11:551–5. https://doi.org/10.1038/s41561-018-0161-1.

[64] Wang S, Zhu X, Song D, Wen Z, Chen B, Feng K. Drivers of CO_2 emissions from power generation in China based on modified structural decomposition analysis. J Clean Prod 2019;220:1143–55. https://doi.org/10.1016/j.jclepro.2019.02.199.

[65] Zhang M, Liu X, Wang W, Zhou M. Decomposition analysis of CO_2 emissions from electricity generation in China. Energy Policy 2013;52:159–65. https://doi.org/10.1016/j.enpol.2012.10.013.

[66] Karmellos M, Kopidou D, Diakoulaki D. A decomposition analysis of the driving factors of CO_2 (Carbon dioxide) emissions from the power sector in the European Union countries. Energy 2020;94:680–92. https://doi.org/10.1016/j.energy.2015.10.145.

[67] Ang BW. LMDI decomposition approach : A guide for implementation. Energy Policy 2015;86:233–8. https://doi.org/10.1016/j.enpol.2015.07.007.

[68] Ang BW, Zhang FQ, Choi K. FACTORIZING CHANGES IN ENERGY AND ENVIRONMENTAL INDICATORS THROUGH DECOMPOSITION. Energy 1998;23:489–95.

[69] Ang BW, Ã NL. Handling zero values in the logarithmic mean Divisia index decomposition approach. Energy Policy 2007;35:238–46. https://doi.org/10.1016/j.enpol.2005.11.001.

[70] Pazheri FR, Othman MF, Malik NH. A review on global renewable electricity scenario. Renew Sustain Energy Rev 2014;31:835–45. https://doi.org/https://doi.org/10.1016/j.rser.2013.12.020.

[71] Waters R, Remouit F, Olauson J, Widén J, Lingfors D, Grabbe M, et al. Variability assessment and forecasting of renewables: A review for solar, wind, wave and tidal resources. Renew Sustain Energy Rev 2015;44:356–75. https://doi.org/10.1016/j.rser.2014.12.019.

[72] Bogdanov D, Farfan J, Sadovskaia K, Aghahosseini A, Child M, Gulagi A, et al. Radical transformation pathway towards sustainable electricity via evolutionary steps Radical transformation pathway towards sustainable electricity via evolutionary steps. Nat Commun n.d.:1–16. https://doi.org/10.1038/s41467-019-08855-1.

[73] Lin J. Rapid cost decrease of renewables and storage accelerates the decarbonization of China's power system. Nat Commun 2010:1–9. https://doi.org/10.1038/s41467-020-16184-x.

[74] Deshmukh R, Phadke A, Callaway DS. Least-cost targets and avoided fossil fuel capacity in India's pursuit of renewable energy. Proc Natl Acad Sci U S A 2021;118. https://doi.org/10.1073/pnas.2008128118.

[75] Wiser R, Rand J, Seel J, Beiter P, Baker E, Lantz E, et al. Expert elicitation survey predicts 37% to 49% declines in wind energy costs by 2050. Nat Energy 2021;6. https://doi.org/10.1038/s41560-021-00810-z.

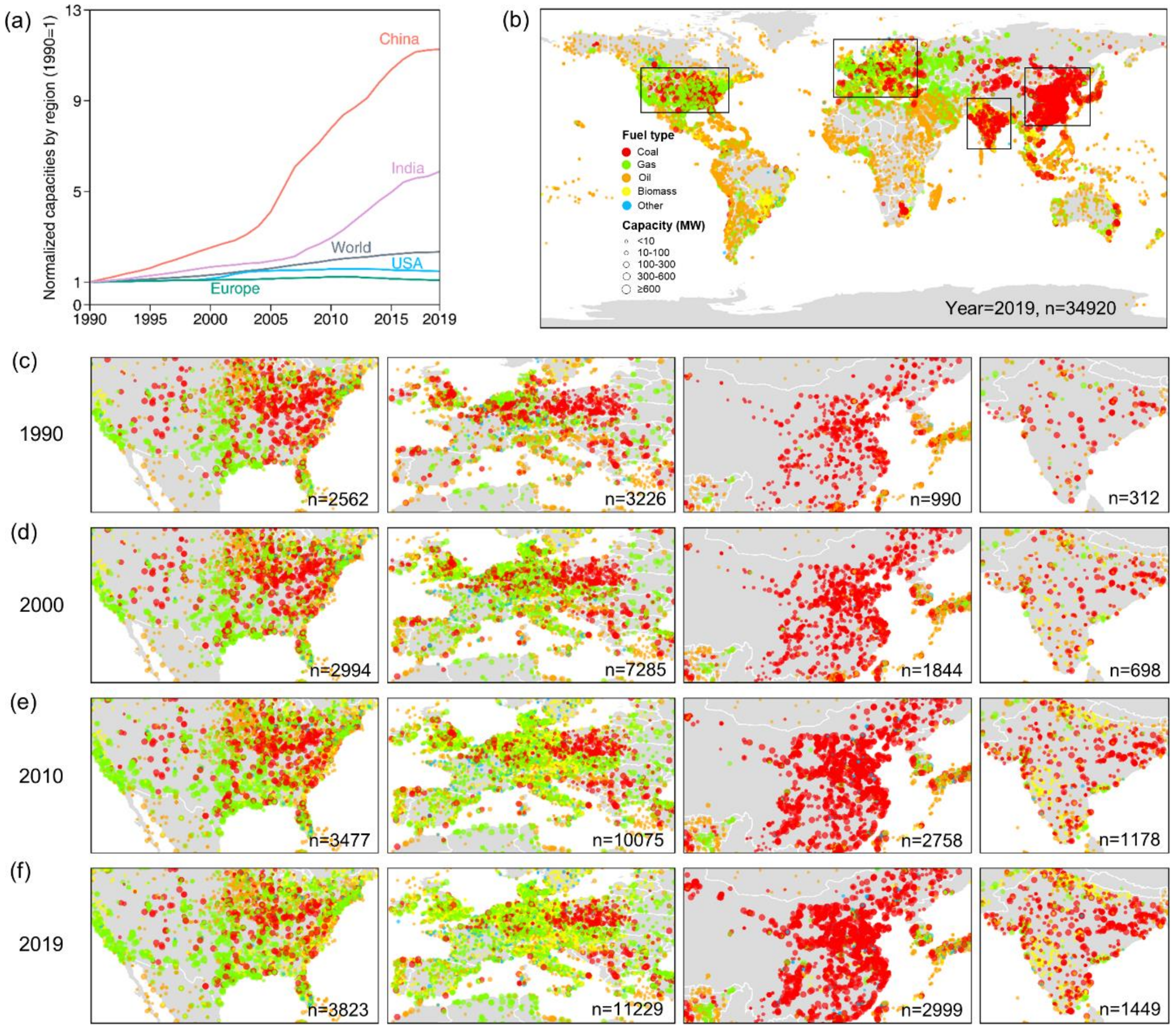

Figure 1. The trend of fossil fuel- and biomass-burning power plant expansion at different scales. (a) Normalized power capacities relative to 1990. The gray lines represent power plant expansion over time at the global scale, and other-colored lines represent expansion patterns by four regions (China, the United States, Europe and India). (b) Spatial distribution of global fossil fuel- and biomass-burning power plants in 2019, colored by fuel type (coal, gas, oil, biomass and others) and classified as nameplate capacity (< 10 MW, 10–100 MW, 100–300MW, 300–600 MW, ≥ 600 MW). (c), (d), (e) and (f) depict the regional spatial distribution in 1990, 2000, 2010 and 2019, respectively, and regional maps from left to right represent the spatial distribution of the United States, Europe, China and India, respectively.

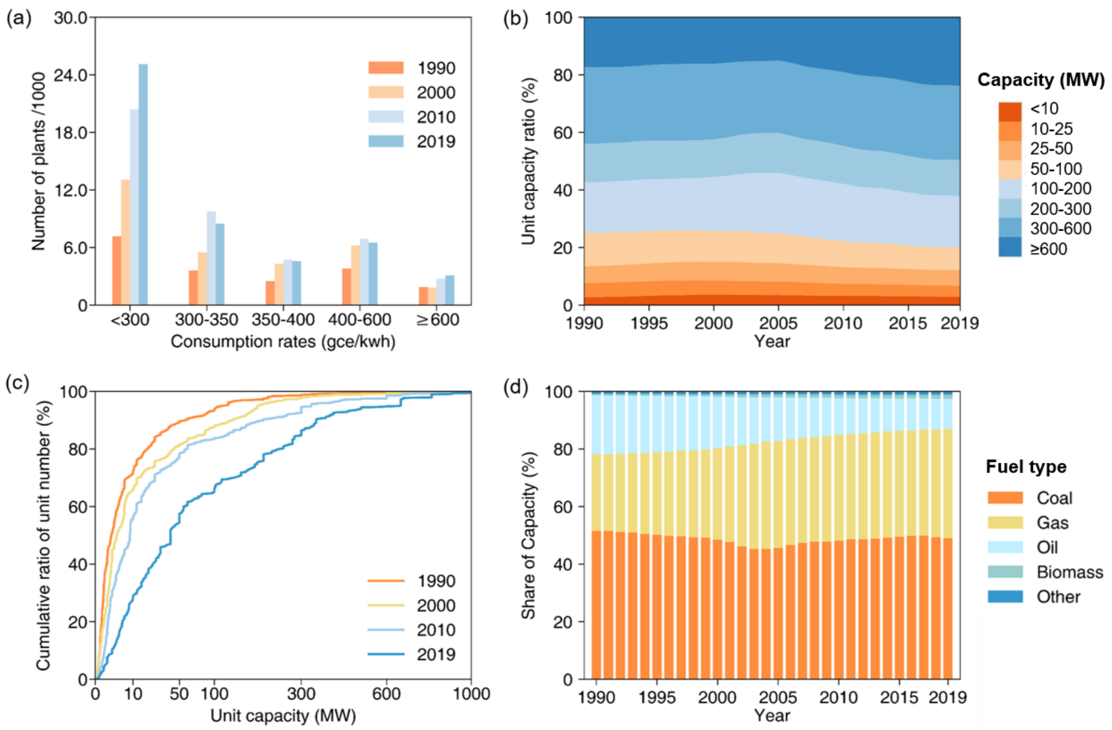

Figure 2. Changes in fleet structure of global power plants from 1990 to 2019. (a) Distribution of coal consumption rates in fossil fuel- and biomass-burning power plants in 1990, 2000, 2010 and 2019. (b) Trends in capacity mix by capacity during 1990–2019. (c) Cumulative ratio of unit number for newly constructed power units for 1990, 2000, 2010 and 2019. The units are sorted according to ascending capacity along the x axis. (d) Trends in capacity mix by fuel type during 1990–2019.

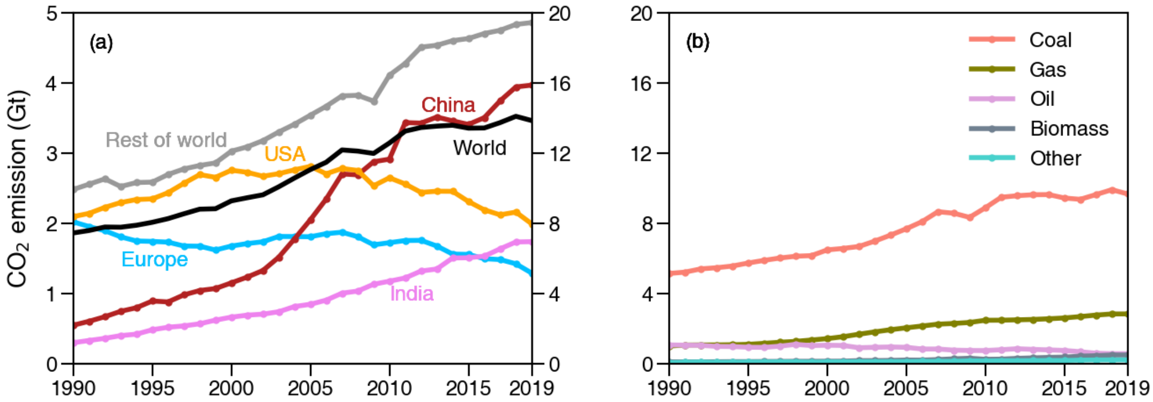

Figure 3. CO_2 emissions of global power plants by region and by fuel type from 1990 to 2019. (a) CO_2 emissions trends at the global and regional scales. (b) Emissions by fuel type, including coal, oil, gas, biomass and other fuel types.

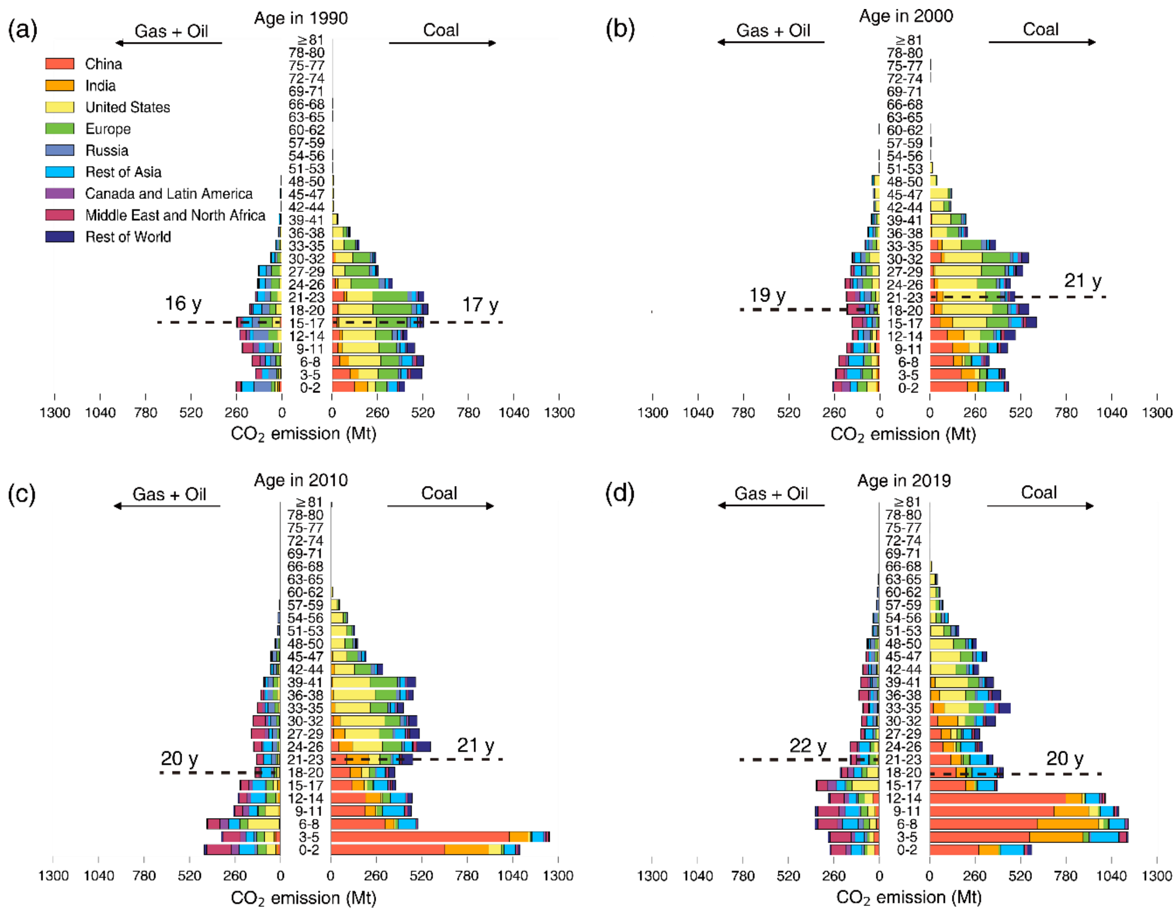

Figure 4. Age structure of CO_2 emissions for global power units in 1990 (a), 2000 (b), 2010 (c) and 2019 (d). Each figure represents the CO_2 emissions of coal-fired units versus gas- and oil-fired units by age distribution. The average age of power units is represented as dotted lines. Note that 0 years old means that power units began operating in that year. See Fig. S2 for the definitions of regions.

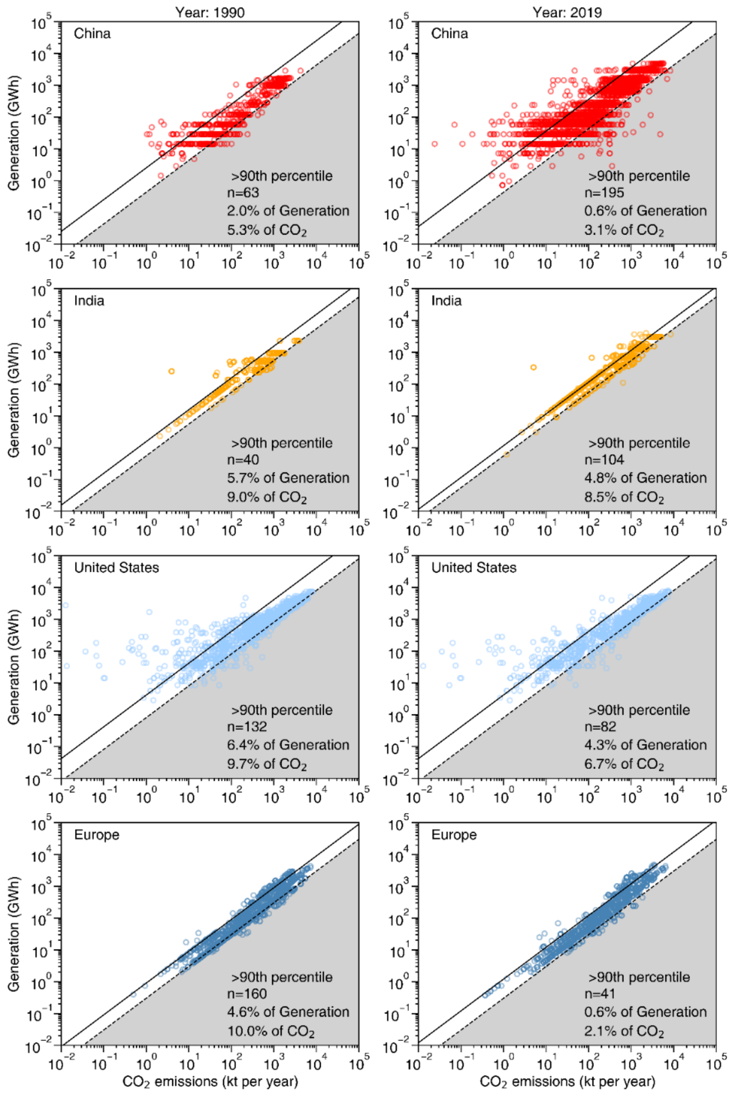

Figure 5. The evolution of low-efficiency coal units between 1990 and 2019. The data points represent individual coal-fired units in China, India, Europe, and the United States, in each case plotted according to power generation (y axis) and annual CO_2 emissions (x axis). Panels are organized by region (rows) and operating year (columns). Diagonal lines indicate the emission intensity (tonnes CO_2 per MWh), and solid diagonal lines represent the 10th percentile values of the emission intensity (tonnes CO_2 per MWh) in the corresponding year. Shaded triangles illustrate units whose emission intensity is over the 90th percentile values of emission intensity.

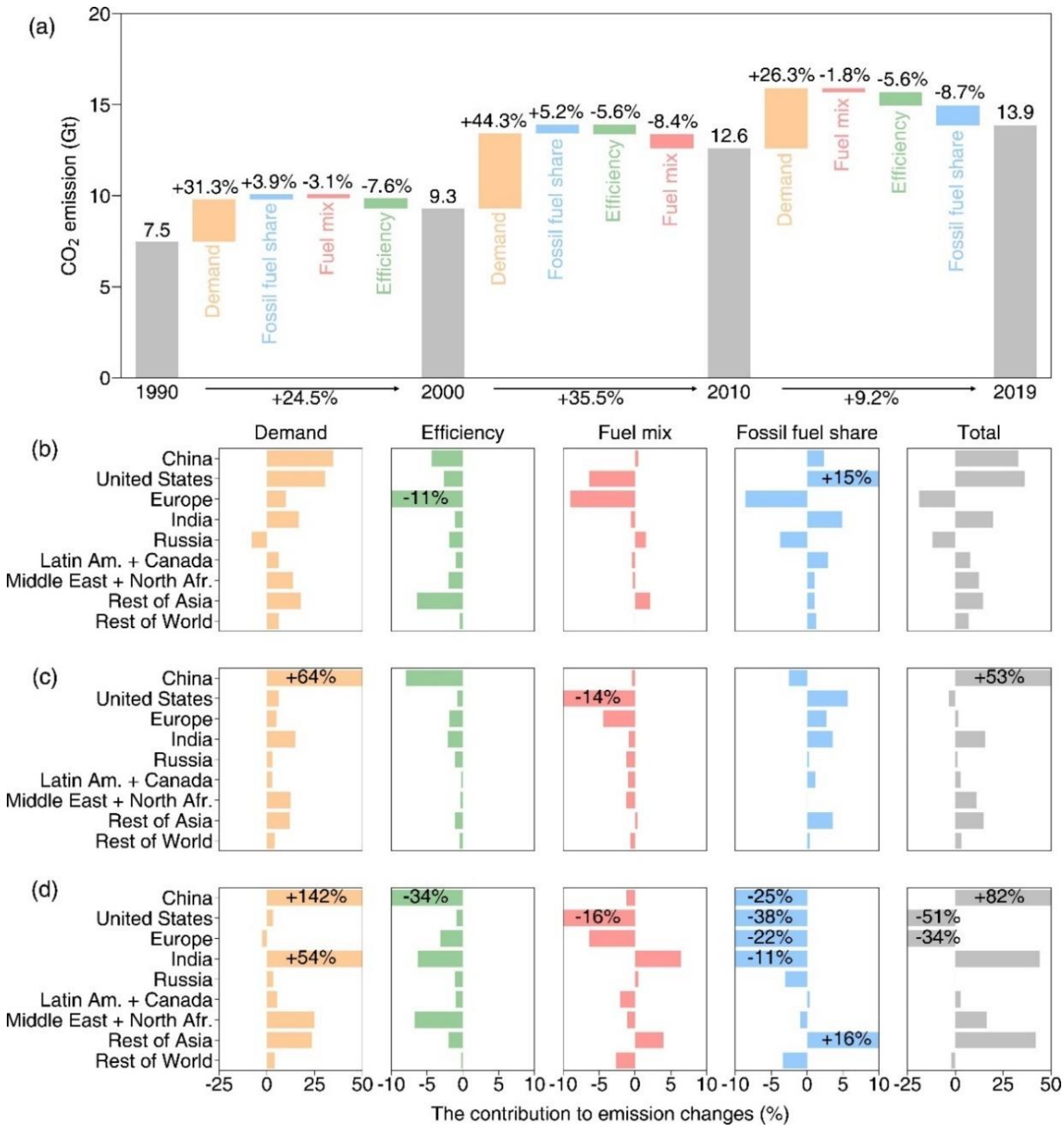

Figure 6. Contribution of each driver and nine regions to the change in the CO_2 emissions of global power plants from 1990 to 2019. (a) Contribution of each driver (power generation demand, energy efficiency, fuel mix and fossil fuel share) to the change in the CO_2 emissions of global power plants in the 1990–2000, 2000–2010 and 2010–2019 periods. The length of each bar reflects the contribution of each factor per year. (b), (c) and (d) represent the regional contributions to emission changes by different drivers in the 1990–2000, 2000–2010 and 2010–2019 periods, respectively.

Supplementary Information

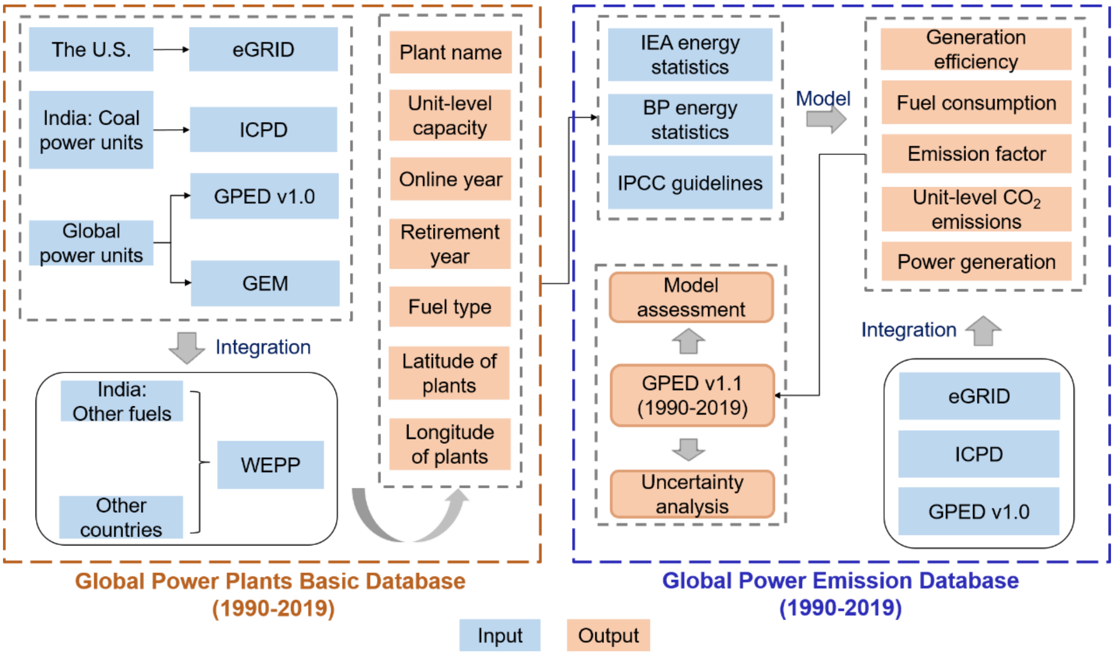

Figure S1. Diagram of global power plants CO_2 emissions database construction.

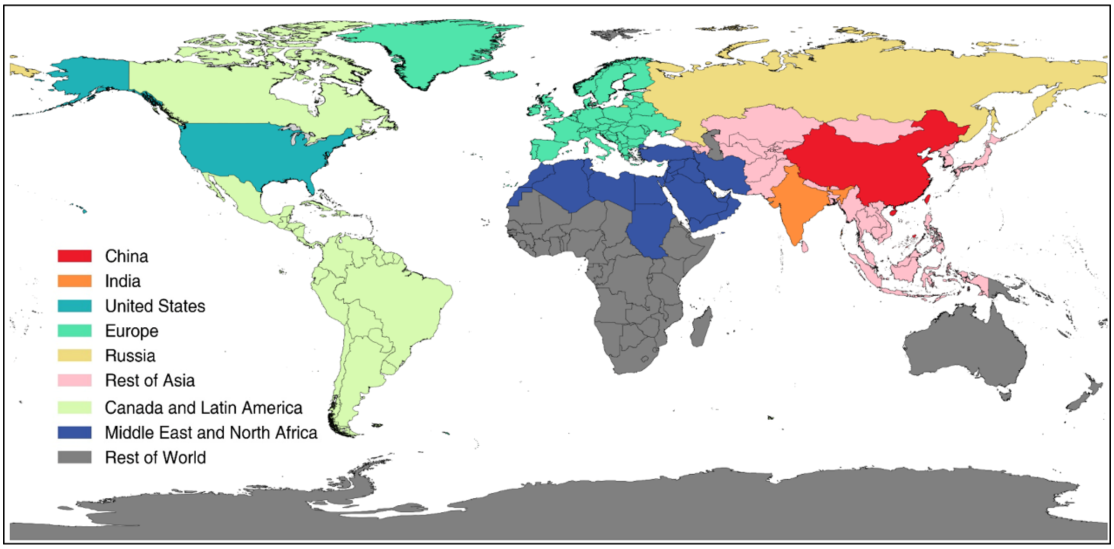

Figure S2. Definition of the nine regions in this study.

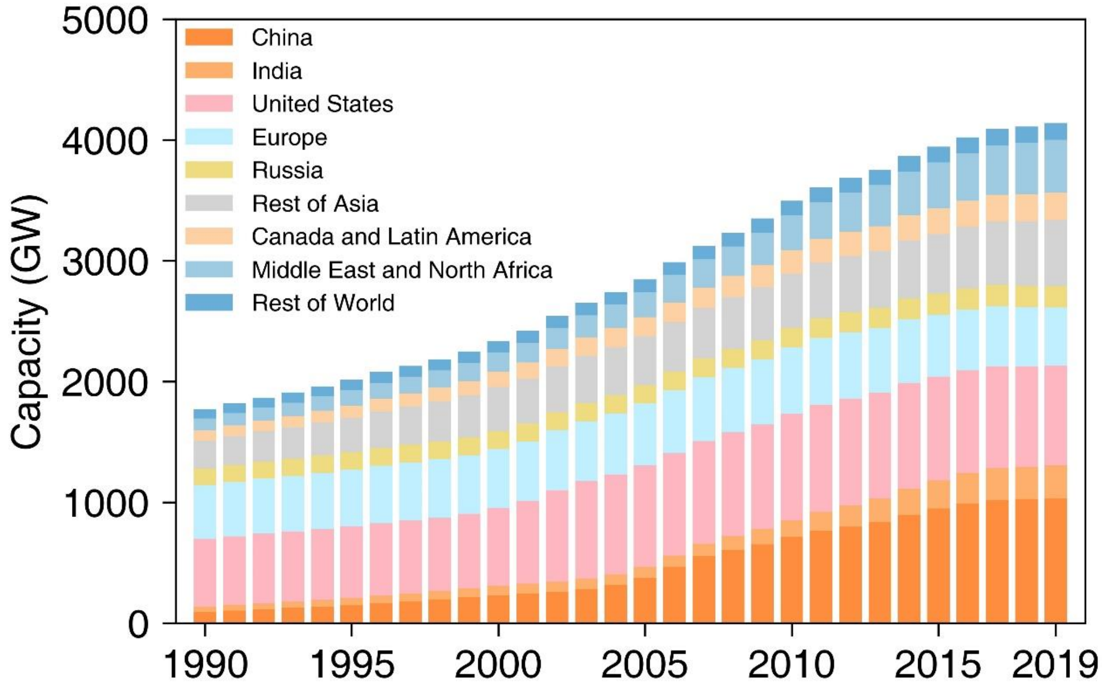

Figure S3. Capacity trends of global operating fossil fuel- and biomass-burning power plants by region from 1990 to 2019.

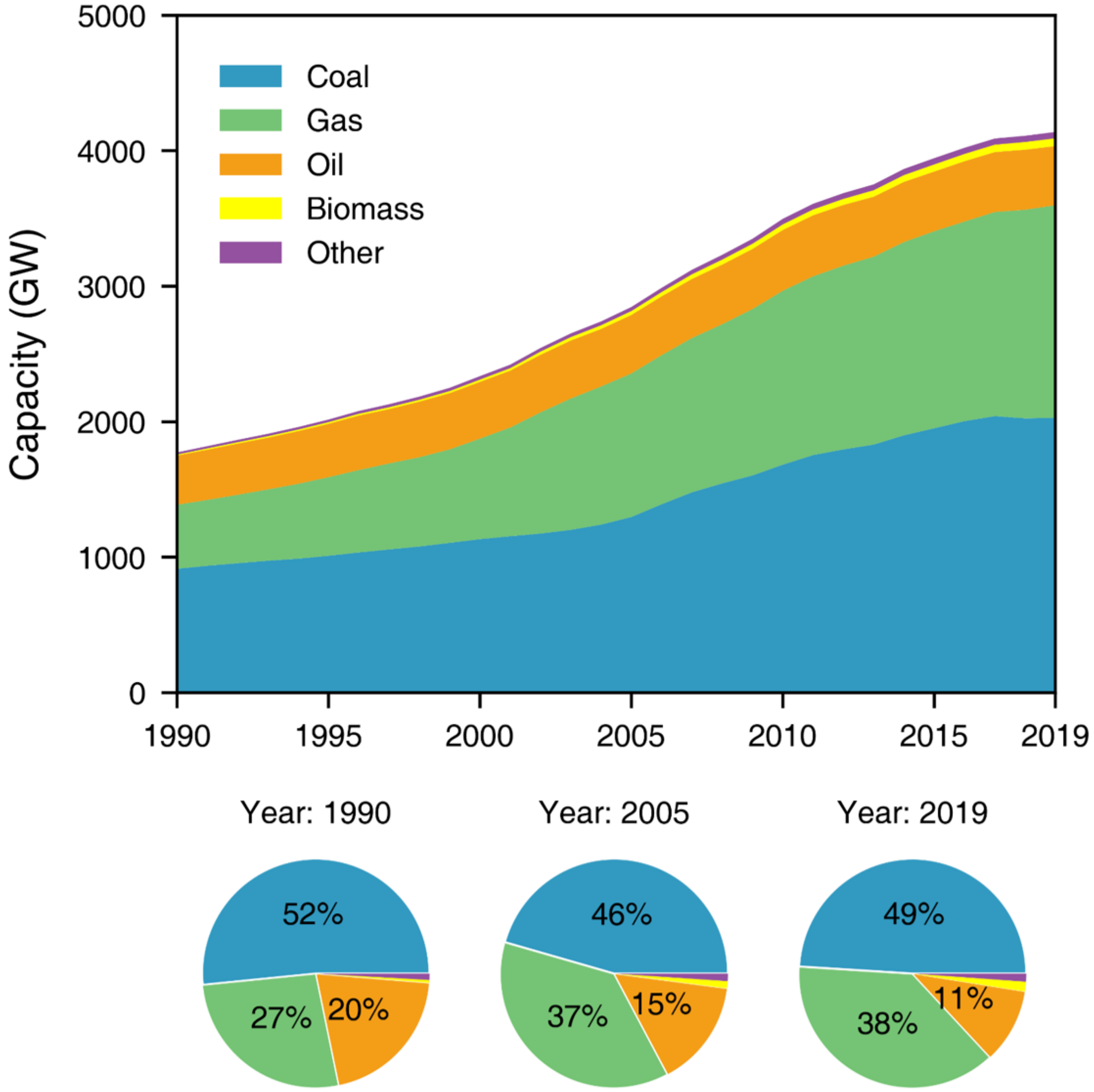

Figure S4. Capacity of global power plants by fuel types during 1990-2019. The stacked chart above represents the capacity trend of coal, natural gas, oil, biomass and other fuel types power plants in 1990-2019. Three pie charts below illustrate global capacity structure by fuel types in 1990, 2005 and 2019.

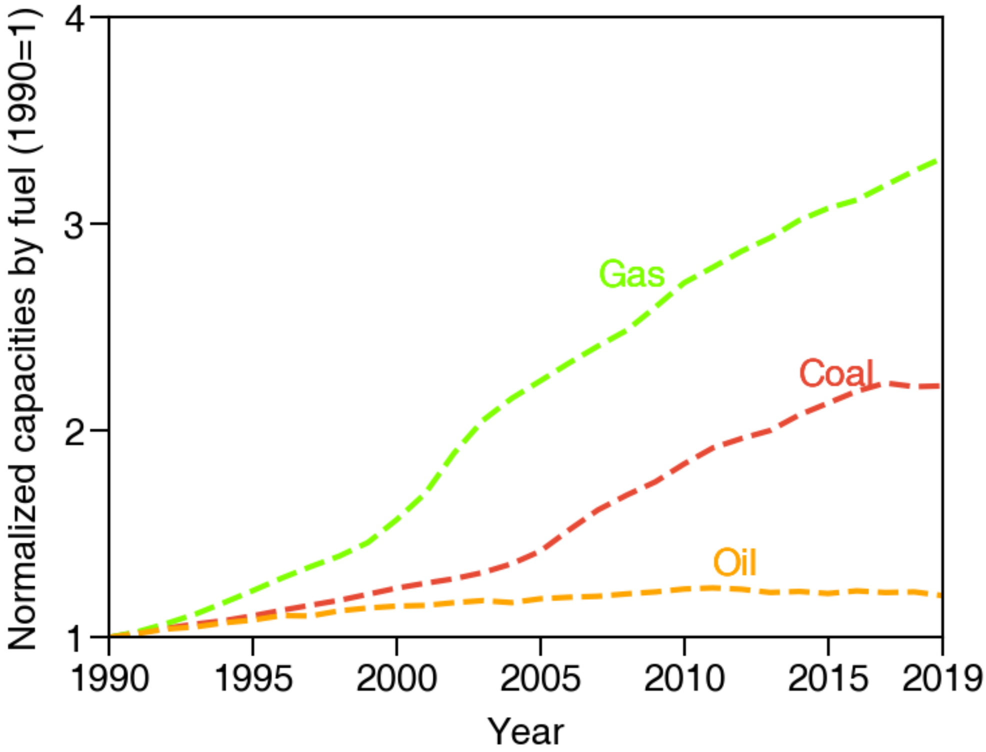

Figure S5. Normalized capacities of global coal-fired, natural gas-fired and oil-fired power plants relative to 1990.

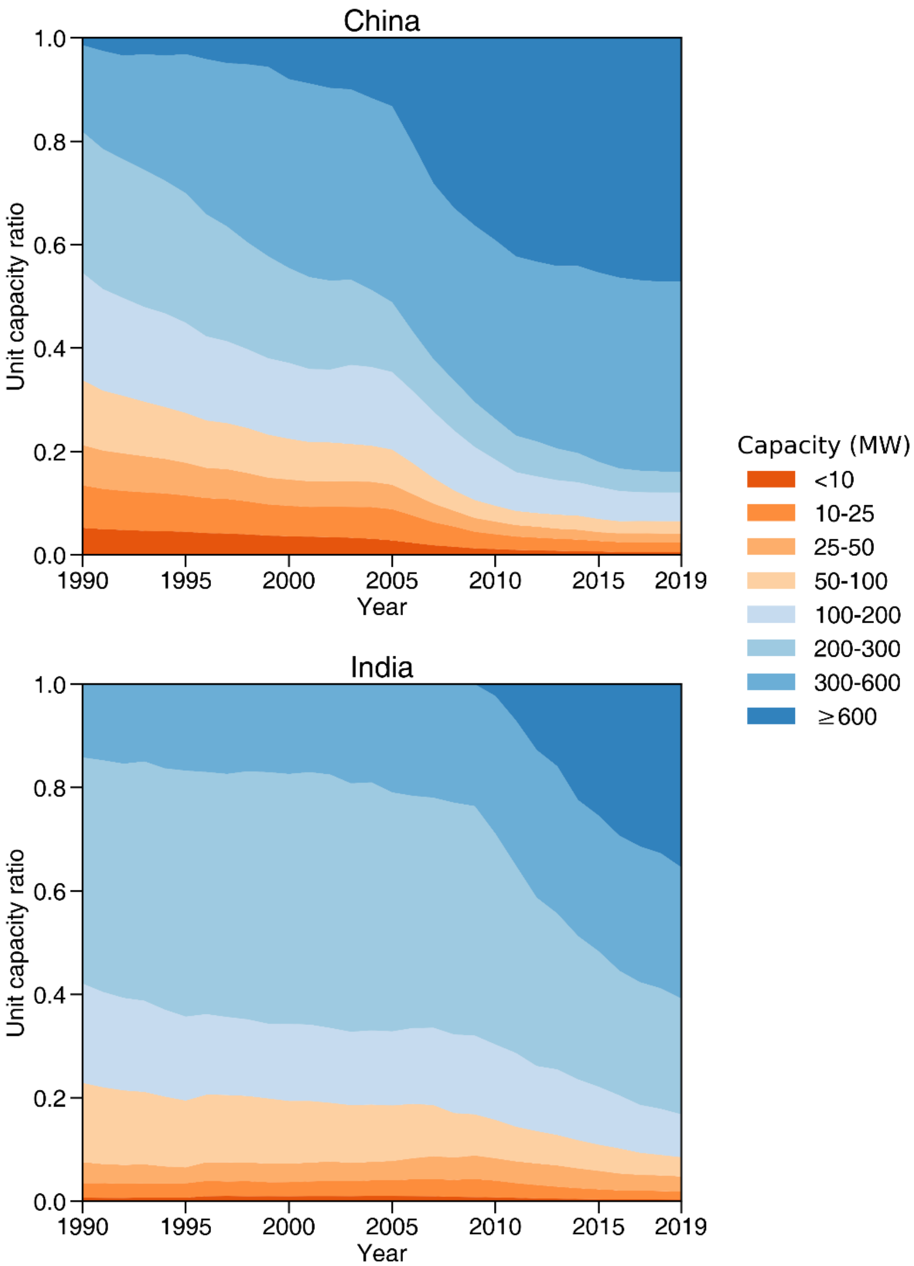

Figure S6. Trends in capacity mix of China and India by capacity size during 1990–2019.

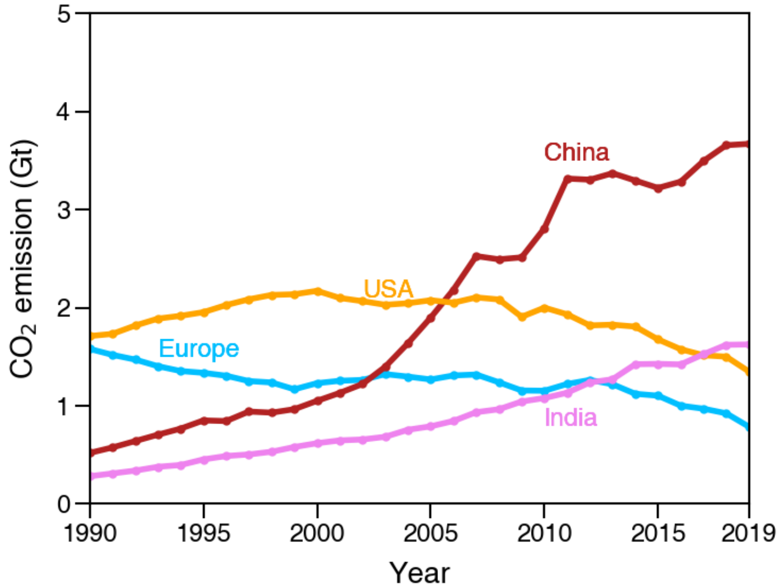

Figure S7. CO_2 emissions trends of coal power plants in China (the salmon line), India (the violet line), the United States (the orange line) and Europe (the blue line) from 1990 to 2019.

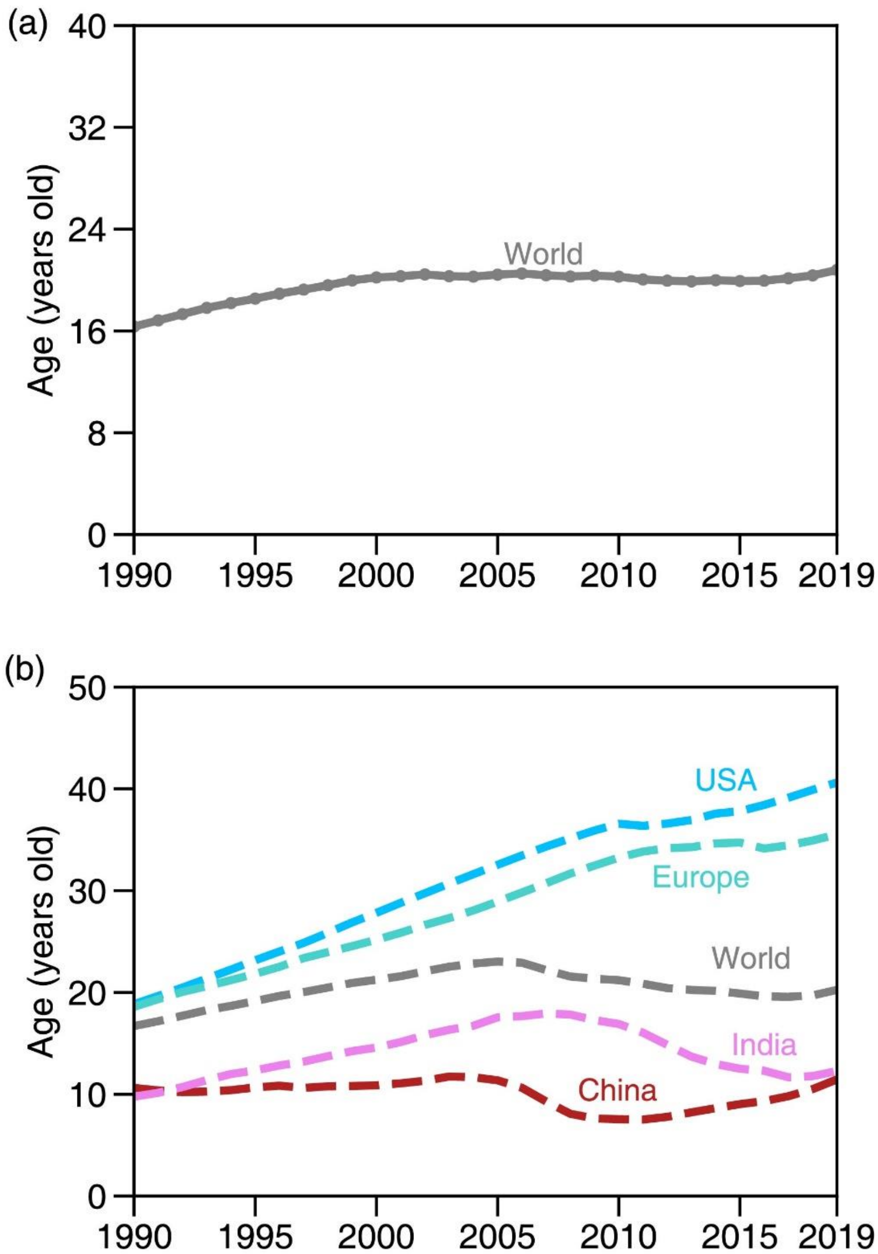

Figure S8. Age trends of global power plants from 1990 to 2019. (a) represents age of global operating thermal power plants. (b) depicts the age trend of operating coal power plants at the global scale (grey dash line) and at key region (China, India, the United States and Europe).

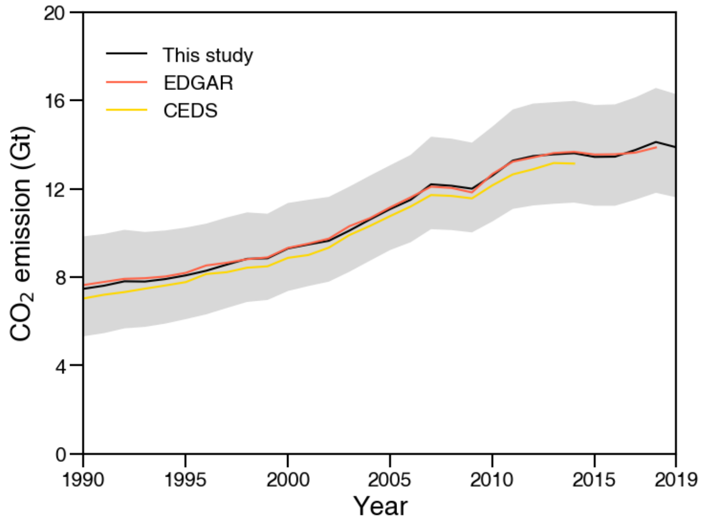

Figure S9. Comparisons of CO_2 emissions from global power plants during 1990-2019. The shaded ranges illustrate the uncertainty range of the 95% CI calculated in this study.